

# Newly Synthesised Gadolinium bis-Phthalocyanine Sandwich Complex: Ambipolar Organic Semiconductor

Seema Barard<sup>1</sup>, Theo Kreouzis<sup>1</sup>, Andrew N. Cammidge<sup>2</sup>, Michael J. Cook<sup>2</sup> and Asim K. Ray<sup>1</sup>

<sup>1</sup>Centre of Materials Research, Queen Mary University of London, Mile End Road, London  
E1 4NS, UK

<sup>2</sup>School of Chemistry, University of East Anglia, Norwich, NR4 7TJ, UK

## ABSTRACT

Time of flight (TOF) photocurrent transient studies on 5µm thick solution processed films of novel non-peripherally octa-octyl-substituted liquid crystalline gadolinium bis-1,4,8,11,15,18,22,25-octakis(octyl) phthalocyanines (8GdPc<sub>2</sub>) provide a quantitative analysis of the intrinsic ambipolar charge transport relative to mesomorphic structure of this lanthanide compound. Characteristic liquid crystalline phases of these molecules have been identified from differential scanning calorimetry supported by observation from the UV-visible absorption, showing crystal-columnar mesophase and columnar mesophase-isotropic liquid transitions at 64.2°C and 162°C, respectively. The TOF carrier mobility is found to be structure dependent and highest values of  $4.73 \times 10^{-6} \text{ m}^2/\text{Vs}$  and  $1.6 \times 10^{-6} \text{ m}^2/\text{Vs}$  have been estimated for hole and electron mobilities for hexagonally packed, columnar structures of the spin-coated films. These results are exploitable for development of single molecule based all organic complimentary analogue and digital circuits with tunable field effect performance.

Key words: Discotic liquid crystalline; time of flight; drift mobility, Poole-Frankel effect; field-lowering coefficient

## 1 Introduction:

Thermally stable phthalocyanine macrocyclic compounds are known to exhibit electrical semiconductivity properties, stimulating active fundamental research interest for a wide range of applications in organic and flexible electronics.<sup>[1]</sup> Lanthanide bis-phthalocyanine sandwich compounds are characterised by their free radical character which facilitates electron transfer from one macrocycle to another due to overlap of  $\pi$ -orbitals.<sup>[2]</sup> Unsubstituted lutetium bis-phthalocyanine (LuPc<sub>2</sub>) is believed to be the first intrinsic molecular semiconductor with room temperature steady state conductivity of  $6 \times 10^{-2} \text{ Sm}^{-1}$ .<sup>[3,4]</sup> Substituted liquid crystalline LuPc<sub>2</sub> molecules with eight long alkyl chains exhibit ordered liquid crystalline mesomorphic properties over temperature range between 100K and 500K and the carriers hopping between the columns is found to be responsible for the frequency conductivity between  $10^{-3} \text{ Hz}$  and  $10^5 \text{ Hz}$ .<sup>[5]</sup> A drift mobility of  $2 \text{ cm}^2\text{V}^{-1} \text{ s}^{-1}$  is reported from in-plane conduction through evaporated LuPc<sub>2</sub> thin films between two gold electrodes.<sup>[6]</sup> The localisation of  $\pi$ -electrons on one of its two macrocycles produces The Heisenberg type paramagnetic behavior of LuPc<sub>2</sub> molecules.<sup>[7]</sup> Following the initial research carried out on LuPc<sub>2</sub> compounds, other rare-earth bisphthalocyaninate compounds such as dysprosium (Dy), europium (Eu), gadolinium (Gd), praseodymium (Pr), terbium (Tb), ytterbium (Yb) have since been investigated for their uses in resistive, optical, electrochemical, impedance or mass sensors.<sup>[8-10]</sup>

Recent applications of plastic electronics are based on those derivatives bearing substituents that confer both solubility in organic spreading solvents and columnar liquid crystal behaviour typically at elevated temperatures. The conductivity of spin-coated thin films of octa(13,17-dioxanonacosane-15-sulfanyl)-substituted mesomorphic LuPc<sub>2</sub> is found to decrease by four orders of magnitude on annealing to 140°C for 3h due to formation of a staggered slipped stacking structure.<sup>[11]</sup> Anthracene doping of up to wt. 5% into spin coated films of octakis(alkylthio) substituted Lu bisphthalocyanine is reported in recent years to increase the

conductivity by two orders of magnitude with simultaneous decreases in activation energy.<sup>[12]</sup> Spin-coated films, ~40nm thick, of alkyl-substituted dysprosium phthalocyanine molecules showed an increase in room temperature Ohmic conductivity by two orders of magnitude from  $6.57 \times 10^{-8} \text{ S m}^{-1}$  to  $6.42 \times 10^{-6} \text{ S m}^{-1}$  as the sample was annealed at the liquid crystalline temperature of 350 K, implying the formation of thermally induced ordered film.<sup>[13]</sup> Values of  $2.12 \times 10^{-7} \text{ m}^2 \text{V}^{-1} \text{ s}^{-1}$ ,  $6.72 \times 10^{-7} \text{ m}^2 \text{V}^{-1} \text{ s}^{-1}$  and  $21.58 \times 10^{-6} \text{ m}^2 \text{V}^{-1} \text{ s}^{-1}$  were estimated for hole mobility of spin-coated tetrasubstituted Lu, Eu, Yb thin films, respectively.<sup>[14]</sup> The Ohmic conductivity of 5 nm thick thermally deposited TbPc<sub>2</sub> under high vacuum conditions is found to be  $0.032 \text{ S m}^{-1}$  at 303 K with the value of 0.158 eV for the temperature independent activation energy, implying the thermal excitation of carriers from a continuous density of deep trap states.<sup>[15]</sup>

This paper reports for the first time bulk ambipolar charge transport in  $5 \mu\text{m}$  thick solution processed films of a novel liquid crystalline gadolinium bis-phthalocyanine complex, 8GdPc<sub>2</sub> in Figure 1, bearing a total of 16 octyl chains ( $\text{R} = \text{C}_8\text{H}_{17}$ ) as substituents on its non-peripheral positions. Thermally induced phase changes were investigated from Differential Scanning Calorimetry (DSC) and UV-vis absorption spectra for bulk materials and spin coated films, respectively. The time of flight (TOF) technique was employed to determine values of electron and hole mobilities  $\mu_e$  and  $\mu_h$  at temperatures below and above the crystal to mesophase transition. This method involved the measurement the time required for a sheet of charge carriers photo-generated near one of the electrodes by pulsed light irradiation to drift across the sample to the other electrode under an applied electric field. In this way it is possible to study the **fastest** charge transport and recombination in organic 8GdPc<sub>2</sub> semiconductors involving the mechanisms within molecules, between molecules, as well as between crystal planes and grains.<sup>[16]</sup> Similarly substituted metal free phthalocyanine molecules (8H<sub>2</sub>Pc) are found to exhibit the unipolar charge transport behaviour with the hole mobility of  $\approx 10^{-4} \text{ m}^2/\text{Vs}$  in the

Col<sub>h</sub> and Col<sub>r</sub> phases. This value is two orders magnitude higher than one obtained in the present case.<sup>[17]</sup>

## 2. Experimental Methods

Synthetic routes to bis-complexes of tetrapyrrole based macrocycles containing a lanthanide metal ion are well established.<sup>[18]</sup> The metal-free 1,4,8,11,15,18,22,25-octakis(octyl)phthalocyanine was reacted with gadolinium acetate under reflux in octanol with 1,8-Diazabicyclo[5.4.0]undec-7-ene (DBU) as a promoter. DSC curves were recorded for as-prepared bulk material 8GdPc<sub>2</sub> over a temperature range between -50°C to 200°C using a Linkam THM600 hot stage, and with a TA Instruments DSC 10 instrument coupled to a TA200 workstation. A polarised light optical microscope (Olympus BH2 polarising microscope with a Linkam THM600 hot stage) was employed to observe corresponding mesophase textures of the molecule. Using a Hitachi U-3000 ultraviolet-visible (UV-vis) spectrometer fitted with a Mettler FP80 processor coupled to a Mettler FP82 hot stage, optical absorption spectra for 8GdPc<sub>2</sub> spun thin films on ultrasonically cleaned quartz substrates were recorded in the 300nm-900 nm at different temperatures to investigate temperature dependent molecular reorganisations. Spin coated films of 8GdPc<sub>2</sub> were prepared by conventional methods using a KW-4A spin coater from the Chemat Technology Inc., USA operating at a rotation speed of 1500rpm for 30 sec. The spreading solution (10 mg/ml) of the 8GdPc<sub>2</sub> compound in chloroform (99.9% anhydrous) was used.

The time of flight (TOF) measurements were performed for determining drift mobilities in a 5  $\mu$ m thick liquid crystal cell with two transparent indium tin oxide (ITO) coated glass electrodes. A liquid crystal cell was placed in a modified Linkam LTS350 hotstage filled with 8GdPc<sub>2</sub> by heating at 185°C, i.e. above the mesophase to isotropic liquid transition temperature. The sample was then cooled at a rate of 2°C/min to help promote larger crystal formation. Antiparallel Polyamide was used as the alignment agent between the organic layer and the ITO

electrodes. The photocurrents were produced using a 532nm pulsed output of a double-frequency Nd:YAG laser. The top and bottom electrodes were connected to an external circuit via a variable resistor and a DC power supply which provided the bias. The resulting photocurrent transient was recorded on a high-resolution digitizing oscilloscope. For the measurement of electron transport, the polarity of the power supply was reversed. Signal averaging and background subtraction were carried out on all signals to improve data quality. Further details on the instrumentation are available from our recent publication.<sup>[19]</sup>

### 3. Results and Discussion

Figure 2 shows structural transitions that occur on the second heating/cooling cycle at temperature  $T$  with enthalpy changes shown in brackets: 64.2 °C (19.4 J/g), 121.6 °C (0.41 J/g), 162.2 °C (3.9 J/g) (Heating-2<sup>nd</sup> cycle), 160.6 °C (5.1 J/g), 121.6 °C (0.56 J/g), 46.4 °C (18.9 J/g). The sharp peak on the heating cycle (lower line) of DSC curve at 64.2 °C is assigned to the transition of the crystal (K) to rectangularly packed columnar mesophase (Col<sub>r</sub>) transition. The small peak, low enthalpy change, at 121.6 °C implies a mesophase to mesophase (Col<sub>r</sub> → Col<sub>h</sub>) transition where h refers to hexagonal packing and that at 162 °C corresponds to melting into the isotropic liquid phase (I). Mesophase types were assigned on the basis of well documented characteristic birefringence textures.<sup>[20]</sup> It is observed from optical pictures in Figure 3 that liquid crystal textures were formed sequentially as the sample was heated. The transition from the columnar rectangular mesophase (Col<sub>r</sub>) to the columnar hexagonal mesophase (Col<sub>h</sub>) was observed. Peripherally octaoctyl-substituted gadolinium phthalocyanine derivatives exhibited similar phase transition from K to Col<sub>r</sub> at 61 °C while Col<sub>r</sub> → Col<sub>h</sub> transition is associated with the temperature of 93 °C.<sup>[21]</sup> However, the thermal behaviour of non-peripherally substituted Pcs is largely determined by the interaction of substituent chains on neighbouring benzo-moieties. The re-arrangement of molecular packing takes place within

the bulk structure of films of these compounds on thermal annealing leading to enhanced electrical characteristics. [22]

UV-vis spectra in Figure 4 show Soret and Q-bands in the range between 340nm and 360 nm, and 640 nm and 730 nm, respectively due to long range face-to-face stacking arrangements of the monomers. The absorption at 490nm is generally associated with the free radical structure of a typical bis-phthalocyanine sandwich compounds. The broad band at 318 nm is assigned to the B band ( $\pi$ - $\pi^*$ ) absorption and it is one of the characteristics absorption bands for bis phthalocyanine. According to the extended Hückel molecular orbital model, doubly degenerate

lowest unoccupied molecular orbital (LUMO) is believed to have centered on the pyrrole and isoindole nitrogen. The interactions between the macrocyclic rings split the  $\pi$  highest occupied molecular orbital (HOMO) levels in the lanthanide sandwich complexes [23] The relative energy distance between the bonding HOMO and LUMO levels is estimated to be 1.73 eV.

The radical band at 473 nm (2.62 eV) is the charge transfer band from the inner doubly degenerate orbital of  $e_1$  to half-filled  $a_2$  orbital. These optical transitions are schematically

described in Figure 4(b) in terms of energy level corresponding to singly degenerate orbitals and doubly degenerate orbitals. The spectral characteristics of are broadly in keeping with

ones observed for quasi-Langmuir-Shafer films of peripherally substituted bis(phthalocyaninato) holmium complexes. [24] The spectra at room temperature (rt) and 35°C are identical, exhibiting the Q-band absorptions at 726nm and 642nm. At 70°C, i.e. within the first mesophase ( $Col_r$ ) range, the band at 726nm has sharpened and exhibits an increase in intensity. The band at 642nm shifts to 640nm, showing a smaller increase in intensity. At 130°C, corresponding to the second mesophase range ( $Col_h$ ), the band at 726nm has undergone small decrease in intensity with the 640nm band returning to 642nm.

Figure 5 (a) shows hole photocurrents on double logarithmic scales at 30°C, 70°C and 130°C for the bias of  $V_a = +30V$ . The transit time  $t_0$  of photo generated carriers corresponding to

the respective inflection points determined by the intersection of the tangents to the initial and post flight parts of the curves and clear inflection points,  $t_0$ , can be observed at 3.18 $\mu$ s, 5.33 $\mu$ s and 1.76 $\mu$ s. The traps for two types of carriers can be distinguished by changing the polarity of bias.<sup>[25]</sup> Therefore, electron transport was also investigated in a single experiment for the same sample for reverse bias of  $V_a = -30V$  and values of 26.5 $\mu$ s, 17.80 $\mu$ s and 5.21 $\mu$ s were obtained for  $t_0$  at the corresponding temperatures from Figure 5(b). The primarily dispersive nature of transport for both types of carriers is consistent with the multidomain film structures which consist of many boundaries. The measurements at room temperature were repeated and values of  $\mu_{(e)}$  and  $\mu_{(h)}$  were estimated at temperature T from the knowledge that

$$\mu_{(e,h)}(T,E) = \frac{d^2}{t_0 V_a} \quad (1)$$

where the film thickness  $d = 5\mu m$ , electric field  $E = \frac{V_a}{d}$ .

The measurements were repeated at room temperature and the results of mean calculations have been summarised in Table I. Both electron and hole mobilities are critically dependent of the mesophase of the 8GdPc<sub>2</sub> films. The mobilities of both carriers in Col<sub>h</sub> mesophases are found to be higher by factor of  $\approx 3$  than those in Col<sub>r</sub> mesophases. TOF measurements were performed on solution processed liquid crystalline metal free phthalocyanine molecules with octahexyl (C<sub>6</sub>H<sub>13</sub>) substitution on similar non-peripheral positions, showing similar mesophase behavior. High drift motilities of up to 1.4 cm<sup>2</sup>V<sup>-1</sup> s<sup>-1</sup> and 0.5 cm<sup>2</sup> V<sup>-1</sup> s<sup>-1</sup> for both hole and electrons in the crystalline solid phase of (6PcH<sub>2</sub>) were obtained at room temperature from the time of flight measurement.<sup>[26]</sup> The mobility values of 8GdPc<sub>2</sub> are at least one order of magnitude higher than those reported for non-peripherally octahexyl substituted ambipolar zinc (ZnPc<sub>6</sub>) phthalocyanine.<sup>[27]</sup>

Values of  $4 \times 10^{-9} m^2 V^{-1} s^{-1}$  and  $8 \times 10^{-10} m^2 V^{-1} s^{-1}$  which have recently been reported for the field effect electron and hole mobilities, respectively of ambipolar Gd-bisphthalocyanine active

layer deposited on silicon substrates by vacuum sublimation are significantly smaller than those obtained from the present TOF measurements.<sup>[28]</sup> Similarly the holes and electrons mobility of  $0.11 \text{ cm}^2 \text{ V}^{-1} \text{ s}^{-1}$  for and  $0.06 \text{ cm}^2 \text{ V}^{-1} \text{ s}^{-1}$ , respectively were obtained for the solution processed quasi-Langmuir-Shäfer film of homoleptic sandwich-type tris[2,3,9,10,16,17,23,24-octa(naphthoxy)phthalocyaninato] europium triple-decker complex as an active layer in the organic field effect transistor (OFET).<sup>[29]</sup> However, the carriers are often injected from the contacts into the channels of OFET transistors and values of OFET mobilities are likely to be limited because of the injection of carries from the contact into the channel.<sup>[30]</sup> Values of 0.15 to  $0.35 \text{ cm}^2 \text{ V}^{-1} \text{ s}^{-1}$  for one-dimensional intracolumnar carrier mobility were reported for liquid crystalline thioalkylated Lu, Eu, Tb bisphthalocyanine using pulse-radiolysis time-resolved microwave conductivity (PR-TRMC) technique.<sup>[31]</sup> The PR-TRMC usually gives larger mobility than TOF because the latter technique involves the transport of charge carriers over relatively large distances in multidomain structures encountering the traps of long life.<sup>[32]</sup> In view of these considerations, the present TOF mobilities represent the realistic ambipolar behaviour of 8GdPc<sub>2</sub> films with potential device applications.

Measurements were repeated between  $10\text{V} \leq V_a \leq 35\text{V}$  with a view to examining the effect of applied field on the mobility. The mobilities of both types of carriers are shown in Figure 6 as function of  $\sqrt{E}$ . The linear relation indicates the Poole-Frankel type field dependence of the mobility at temperature  $T$  in the form;

$$\mu_{(e,h)}(T, E) = \mu_{(e,h)}(T, E = 0) \exp(\beta \sqrt{E}) \quad (2)$$

The errors in  $\mu_{(e,h)}$  primarily arises from the dependence of the electric field  $E$  on thickness  $d$ . the errors in the transit time, are negligibly small. The least square fitting of Equation (2) to experimental data is also included in the error bars.

Values of the field lowering coefficients  $\beta$  are estimated in the order of  $+10^{-5} \text{ m}^{5/2} \text{ V}^3 \text{ s}$  for holes and  $+10^{-6} \text{ m}^{5/2} \text{ V}^3 \text{ s}$  for electrons. The physical interpretation of these positive values of  $\beta$



may be obtained by examining their dependence on the Gaussian density of energy states of width  $\sigma$  and the dimensionless parameter defining the positional disorder  $\Gamma$  through the following form:

$$\beta = 0.78 \sqrt{\frac{qR}{\sigma}} \left[ (\sigma/kT)^{3/2} - \Gamma \right] \quad (3)$$

where  $R$  is the intersite spacing parameter.<sup>[33]</sup> It is obvious from Equation (3) that the positional order  $\Gamma$  is small in comparison with energy states of width  $\sigma$  implying the liquid crystalline GdPc<sub>2</sub> films are well structured. Similar positive field dependent mobility behaviour was observed for liquid-crystalline semiconducting polymers based on poly(2,5-bis(3-alkylthiophen-2-yl)thieno[3,2-b]thiophene).<sup>[34]</sup> The energy state of width for holes in Col<sub>h</sub> mesophases is estimated to 70% narrower than those in Col<sub>r</sub> mesophases from the intercept at  $E=0$  of the Poole-Frankel plots using Equation (4) in the following form:

$$\mu_{(e,h)}(T, E=0) = \mu_{0(e,h)} \exp \left[ - \left( \frac{3}{5} \frac{\sigma}{kT} \right)^2 \right] \quad (4)$$

where  $\mu_{0(e,h)}$  is the carrier mobility in the energetically disorder-free system at  $E = 0$ . Similar calculations have been repeated for electrons and it is found that the energy states for Col<sub>r</sub> mesophases are wider than Col<sub>h</sub> mesophases by more than 200%.

#### 4. Concluding remarks

The synthesis of solution processed liquid crystalline non-peripherally octaoctyl-substituted gadolinium bis-phthalocyanine complex, 8GdPc<sub>2</sub> ambipolar organic semiconductors is important for development of organic complementary metal oxide semiconductor (CMOS) circuits and organic light-emitting transistors. Transition temperatures for phase changes have been well defined by DSC curves and UV-visible absorption spectra. The ambipolar charge transport in 8GdPc<sub>2</sub> compounds is consistent with relative positions of HOMO and LUMO levels derived from optical transitions. The TOF mobilities of both types of carriers which can

be selectively tuned by the annealing temperature of the 8GdPc<sub>2</sub> films are bulk characteristics and therefore these properties may be suitably exploited for design and fabrication of all organic complimentary printable circuits.

### Acknowledgements

The research was financially supported by the UK Technology Strategy Board (Project No. TP/6/EPH/6/ S/K2536J).

### References

1. Gsanger M., Bialas D., Huang L. Z., Stolte M. and Wurthner F. Organic Semiconductors based on Dyes and Color Pigments. *Adv. Mater.* **28(19)** (2016).3615-3645.
2. Padilla, J. and Hatfield, W. E. Correlation between pi-orbital overlap and conductivity in bis-phthalocyaninato lanthanides *Inorg. Chim. Acta* **185(2)** (1991) 131-136
3. Simon J., Andre J. J. and Maitrot M. Lutetium Bisphthalocyanine: The First Molecular Semiconductor. In: Maruani J. (eds) *Molecules in Physics, Chemistry, and Biology. Topics in Molecular Organization and Engineering*, **2** (1988) 599-614 Springer, Dordrecht
4. Turek, P., Petit, P., André, J. J., Simon, J., Even, R., Boudgema, B., Guillaud, G. and Maitrot M., A new series of molecular semiconductors - phthalocyanine radicals .2. *J. Am. Chem. Soc.* **109** (1987) 5119–5122.
5. Belarbi Z., Sirlin C., Simon J. and Andre J. J. Electrical and magnetic-properties of liquid-crystalline molecular materials - lithium and lutetium phthalocyanine derivatives *J. Phys. Chem.* **93(24)** (1989) 8105-8110.
6. Madru, R., Guillaud, G., Alsadoun, M., Maitrot, M. and Schunck, J. P., Mobility experiments on lutetium bisphthalocyanine thin-films.: *Chem. Phys. Lett.* **168 (1)** (1990) 41-44.
7. Petit P. Magnetism of lutetium bisphthalocyanine. *Synth. Met.* **46(2)** (1992) 147-163.
8. Rodriguez-Mendez, M. L., Gay and M. de Saja, J. A. New insights into sensors based on radical bisphthalocyanines. *J. Porphyr. Phthalocyanines* **13(11)** (2009) 1159-1167.
9. Richardson, T., Smith, V. C., Topaclic, A., Jiang, J. and Huang, C. H. In situ visible spectroscopy of an exposed to chlorine gas. *Supramol. Sci.* **4 (3-4)** (1997) 465-470 .

10. Chen, Y. L., Liu, H. G., Pan, N. and Jiang, J. Z. Langmuir-Blodgett films of substituted bis(naphthalocyaninato) rare earth complexes: structure and interaction with nitrogen dioxide . *Thin Solid Films*. **460(1-2)** (2004) 279-285.
11. Basova, T., Kol'tsov, E., Hassan, A. K., Ray, A. K., Gurek, A. G. and Ahsen, V, Effects of structural reorganization in phthalocyanine films on their electrical properties *Mater. Chem. Phys.* **96(1)** (2006) 129-135
12. Hassan, A., Basova, T., Gurek, A. G. and Ahsen, V., Anthracene doping effects on thin films properties of octakis(alkylthio) substituted lutetium bisphthalocyanine *J. Porphyr. Phthalocyanines* **17(6-7)** (2013) 454-459.
13. Basova, T., Grek, A. G. Ahsen, V. and Ray, A. K., Electrical properties of dysprosium phthalocyanine films. *Org. Electron.* **8(6)** (2007) 784-790.
14. Bilgicli, A. T., Gunsul, A., Kandaz, M., Altindal, A. and Comert, H. Highly soluble tetrasubstituted lanthanide bis-phthalocyanines; synthesis, characterization, electrical properties and aggregation studies. *J. Porphyr. Phthalocyanines*. 20(8-11) (2016) 1065-1074.
15. Murdey, R., Katoh, K., Yamashita, M. and Sato, N., Thermally activated electrical conductivity of thin films of bis (phthalocyaninato) terbium (III) double decker complex *Thin Solid Films* **646** (2018) 17-20.
16. Tiwari, S. and Greenham, N. C., Charge mobility measurement techniques in organic semiconductors. *Opt. Quantum Electron.* **41(2)** ((2019) 69-89
17. Miyake, Y., Shiraiwa, Y., Okada, K., Monobe, H., Hori, T., Yamasaki, N., Yoshida, H., Cook, M. J., Fugii, A., Ozaki, M. and Shimizu, Y., High Carrier Mobility up to 1.4 cm<sup>2</sup>V<sup>-1</sup>s<sup>-1</sup> in Non-Peripheral Octahexyl Phthalocyanine. *Appl. Phys. Express* **4 (2)** (2011) 021604.
18. Garland, A. D., Chambrier, I., Cammidge, A. N., and Cook, M. J., Design and synthesis of liquid crystalline phthalocyanines: combinations of substituents that promote the discotic nematic mesophase. *Tetrahedron* **71(39)** (2015) 7310-7314.
19. Barard, S. Heeney, M. Chen, L. Colle, M., Shkunov, M., McCulloch, I., Stingelin, N Philips, M. and Kreouzis, T. Separate charge transport pathways determined by the time of flight method in bimodal polytriarylamine. *J. Appl. Phys.* **105(1)** (2009) **Article Number:** 013701.
20. Cherodian A. S., Davies, A. N., Richardson, R. M., Cook, M. J., McKeown, N. B., Thomson, A. J., Feijoo, J., Ungar, G. and Harrison, K. J. Mesogenic behavior of some

- 1,4,8,11,15,18,22,25-octa-alkylphthalocyanines *Mol. Cryst. Liq. Cryst.* 1991; **196**: 103-114.
21. Zhang Y., Jiang Z., Sun X. and Xue Q., Liquid Crystal Behaviour of 2,3,9,10,16,17,23,24-Octakis(octyloxy)phthalocyanine-containing Gadolinium Sandwich Complexes. *Aust. J. Chem.*, **62** (2009) 455–463.
  22. Chen, Y. L., Li, D. P., Yuan, N., Gao, J., Gu, R. M., Lu, G. F. and Bouvet, M., Tuning the semiconducting nature of bis(phthalocyaninato) holmium complexes via peripheral substituents. *J. Mater. Chem.* **22(41)** (2012) 22142-221.
  23. Rousseau, R., Aroca, R. and Rodriguezmendez, M. L. Extended huckel molecular-orbital model for lanthanide bisphthalocyanine complexes. *J. Mol. Struct.* **356(1)** (1995) 49-62 DOI: 10.1016/0022-2860(95)08905-B
  24. Basova T., Hassan A., Durmus M. Gurek A. G. and Ahsen V., Liquid crystalline metal phthalocyanines: Structural organization on the substrate surface. *Coord. Chem. Rev.* **310** (2016).131-153.
  25. Pavlica E., Bratina G. and Time-of-flight mobility of charge carriers in position-dependent electric field between coplanar electrodes. *Appl. Phys. Lett.* **101(9)** (2012) 093304.
  26. Iino, H., Hanna, J-I., Bushby R. J., Movaghar, B., Whitaker, B. J. and Cook, M. J. Very high time-of-flight mobility in the columnar phases of a discotic liquid crystal. *Appl. Phys. Lett.* **87(13)** (2005) 132102.
  27. Chaure N. B., Barard S., Ray A. K., Cammidge A. N and Cook M. J. Ambipolar charge transport in non-peripherally substituted octahexyl zinc phthalocyanine. *EPL* **104(5)** (2013) 57005.
  28. Kratochvilova, I. Sebera, J. Paruzel, B., Pflieger, J., Toman, P., Maregova, E., Havlova, S., Hubik, P., Buryi, M., Vrnata, M., Slota, R., Zakrzyk, M., Lancok, J. and Novotny, M., Electronic functionality of Gd-bisphthalocyanine: Charge carrier concentration, charge mobility, and influence of local magnetic field. *Synth. Met.* **236** (2018) 68-78.
  29. Kong, X., Lu, G. Zhang, X., Li, X. Y., Chen, Y. L. and Jiang, J. Z. Controlled morphology of self-assembled microstructures via solvent-vapor annealing temperature and ambipolar OFET performance based on a tris(phthalocyaninato) europium derivative. *Dyes Pigment.* **143** (2017) 203-210.
  30. Dost, R. Das, A. and Grell, M. Time-of-flight mobility measurements in organic field-effect transistors. *J. Appl. Phys.* **104(8)** (2008) Article Number: 084519.

31. Ban, K., Nishizawa, K., Ohta, K., de Craats, A. M. V., Warman, J. M., Yamamoto, I. and Shirai, H. Discotic liquid crystals of transition metal complexes 29: mesomorphism and charge transport properties of alkylthio-substituted phthalocyanine rare-earth metal sandwich complexes. *J. Mater. Chem.* **11**(2) (2001) 321-331.
32. van de Craats, A. M., Warman, J. M., deHaas, M. P., Adam, D., Simmerer, J., Haarer, D. and Schuhmacher, P. The mobility of charge carriers in all four phases of the columnar discotic material hexakis(hexylthio)triphenylene: Combined TOF and PR-TRMC results *Adv. Mater.* **8**(10) (1996) 823-826.
33. Hertel D., Bässler H., Scherf U. and Hörhold H. H. Charge carrier transport in conjugated polymers *J. Chem. Phys.* **110**(18) (1999) 9214-9222.
34. Baklar, M., Barard, S., Sparrowe, D., Wilson, R. M., McCulloch, I., Heeney, M., Kreouzis, T. and Stingelin, N. Bulk charge transport in liquid-crystalline polymer semiconductors based on poly(2,5-bis(3-alkylthiophen-2-yl)thieno[3,2-b]thiophene). *Polym. Chem.* **1**(9) (2010) 1448-1452

### Figure captions

**Figure 1:** Chemical structure of non-peripherally octaoctyl-substituted bis-1,4,8,11,15,18,22,25-octakis(octyl) phthalocyaninato gadolinium.

**Figure 2:** Differential scanning calorimetric curves for 8GdPc<sub>2</sub> for heating and cooling cycles.

**Figure 3:** Polarized optical microscopic texture at room temperature after annealing from the isotropic liquid

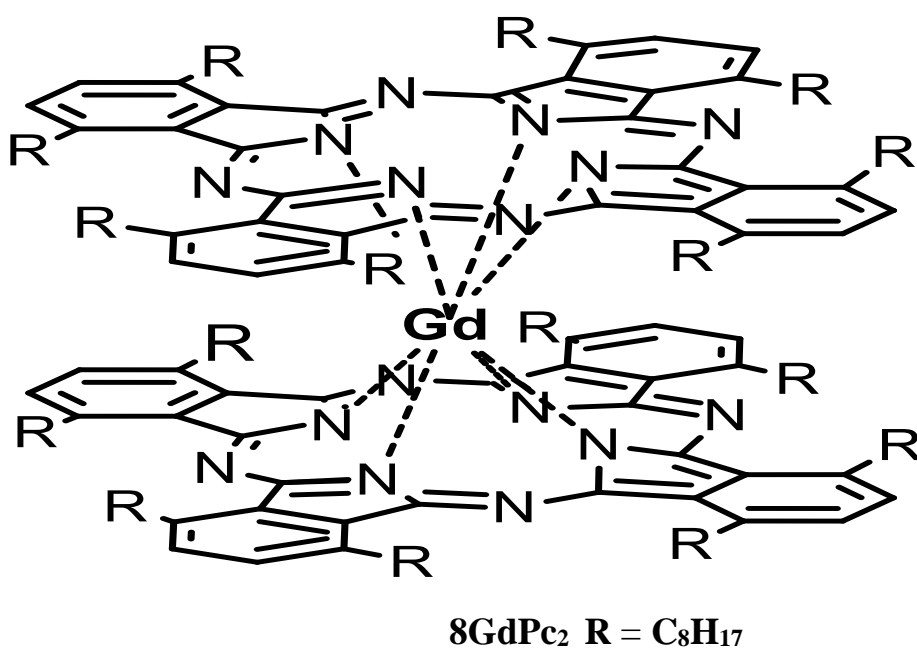
**Figure 4:** (a) UV-visible spectra of 8GdPc<sub>2</sub> film on quartz substrate and (b) room temperature optical transitions (**a<sub>2</sub>→e<sub>1</sub><sup>\*</sup>**), (**b<sub>1</sub>→e<sub>3</sub><sup>\*</sup>**) and (**e<sub>1</sub>→a<sub>2</sub>**) corresponding to 728 nm, 643 nm and radical bands of a spin-coated 8GdPc<sub>2</sub> film, respectively.

**Figure 5:** Hole and Electron photocurrent transients in a 5μm thick cell of 8GdPc<sub>2</sub>.

**Figure 6:** Poole-Frankel plots for (a) hole and (b) electron mobilities in 8GdPc<sub>2</sub>

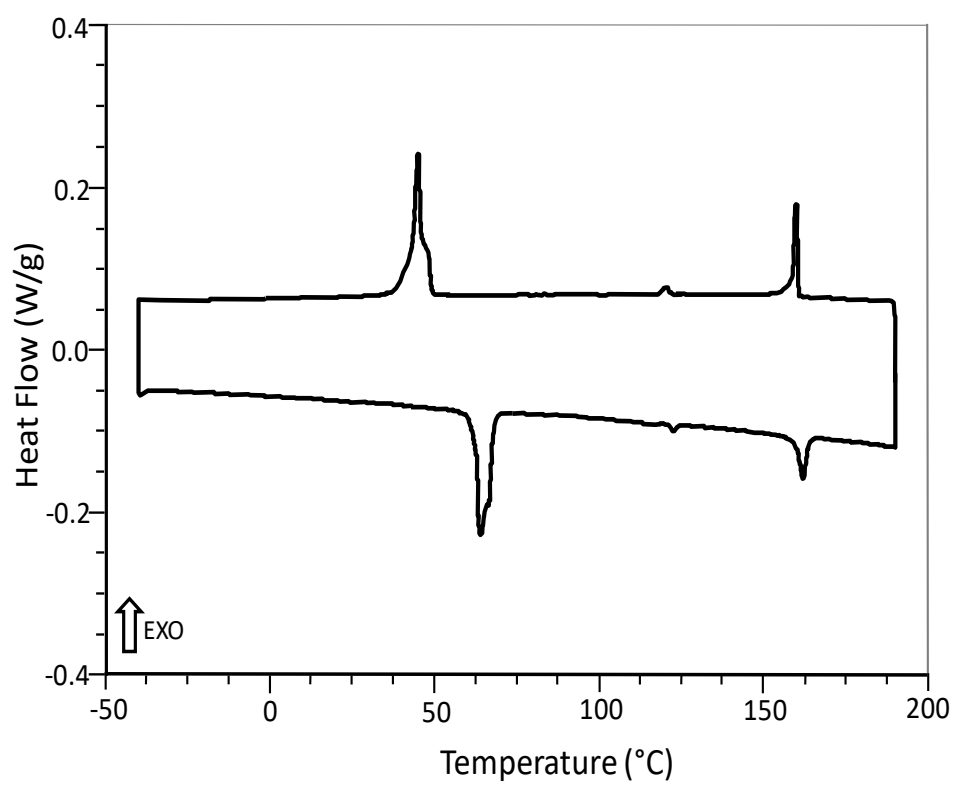
**Table I: Summary of mobility calculations using Equation (1)**

Mesophase	Transition Temperature (°C)	holes		electrons	
		$\tau_o$	$\mu_{(h)}$	$\tau_o$	$\mu_{(e)}$
		( $\mu$ s)	( $10^{-6}\text{m}^2/\text{Vs}$ )	( $\mu$ s)	( $10^{-6}\text{m}^2/\text{Vs}$ )
K	30	3.18	0.262	2.65	0.0341
Col <sub>r</sub>	70	5.33	0.156	17.8	0.0468
Col <sub>h</sub>	130	1.76	0.473	5.21	0.159

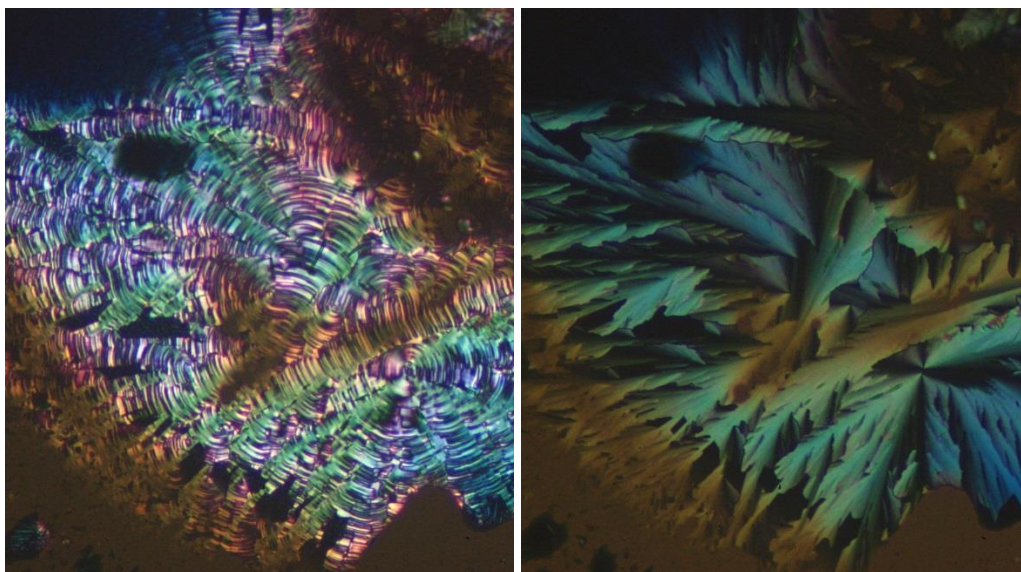


**Figure 1:** Chemical structure of non-peripherally octaoctyl-substituted bis-1,4,8,11,15,18,22,25-octakis(octyl) phthalocyaninato gadolinium

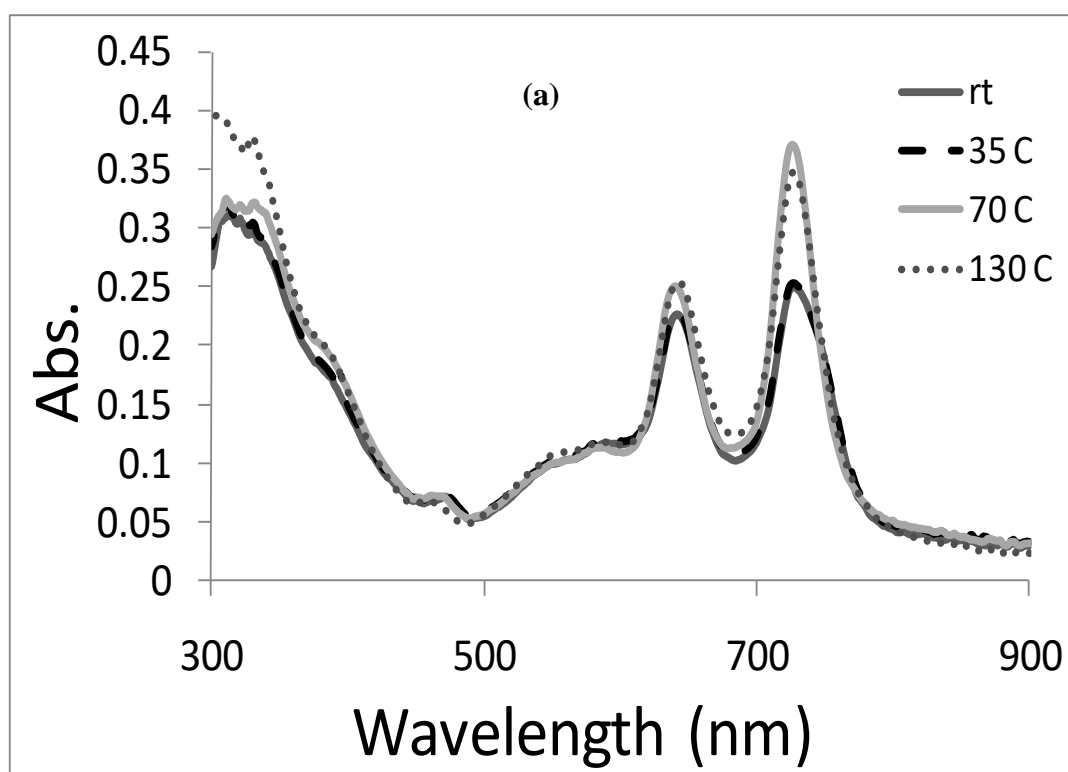




**Figure 2:** Differential scanning calorimetric curves for 8GdPc<sub>2</sub> for heating and cooling cycles.



**Figure 3:** Polarized optical microscopic texture at room temperature after annealing from the isotropic liquid



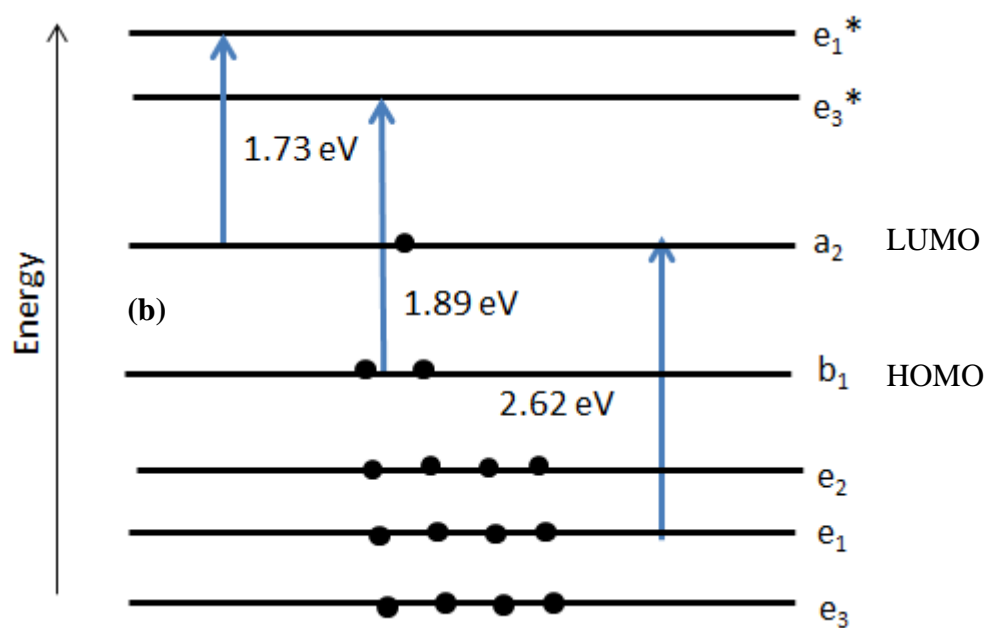


**Figure 4:** (a) UV-visible spectra and (b) room temperature optical transitions between orbitals ( $a_2 \rightarrow e_1^*$ ), ( $b_1 \rightarrow e_3^*$ ) and ( $e_1 \rightarrow a_2$ ) corresponding to 730nm band, 764nm band and radical band of a spin-coated 8GdPc<sub>2</sub> film.

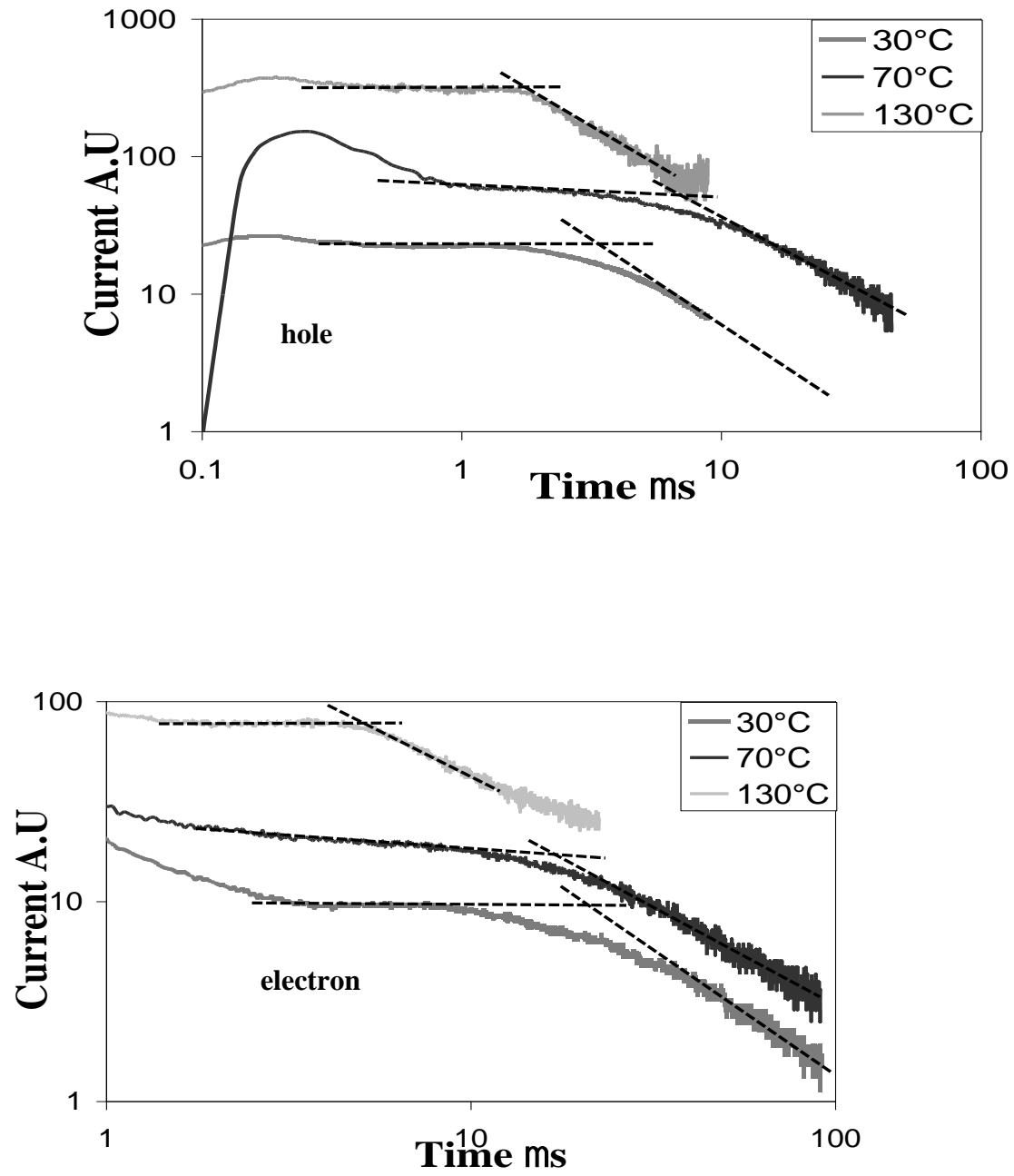


**Figure 5:** Hole and Electron photocurrent transients, measured at room temperature in a  $5\mu\text{m}$  thick cell of 8GdPc<sub>2</sub> for K, Col<sub>r</sub> and Col<sub>h</sub> mesophases corresponding to transition temperature of 30<sup>0</sup>C, 70<sup>0</sup>C and 130<sup>0</sup>C

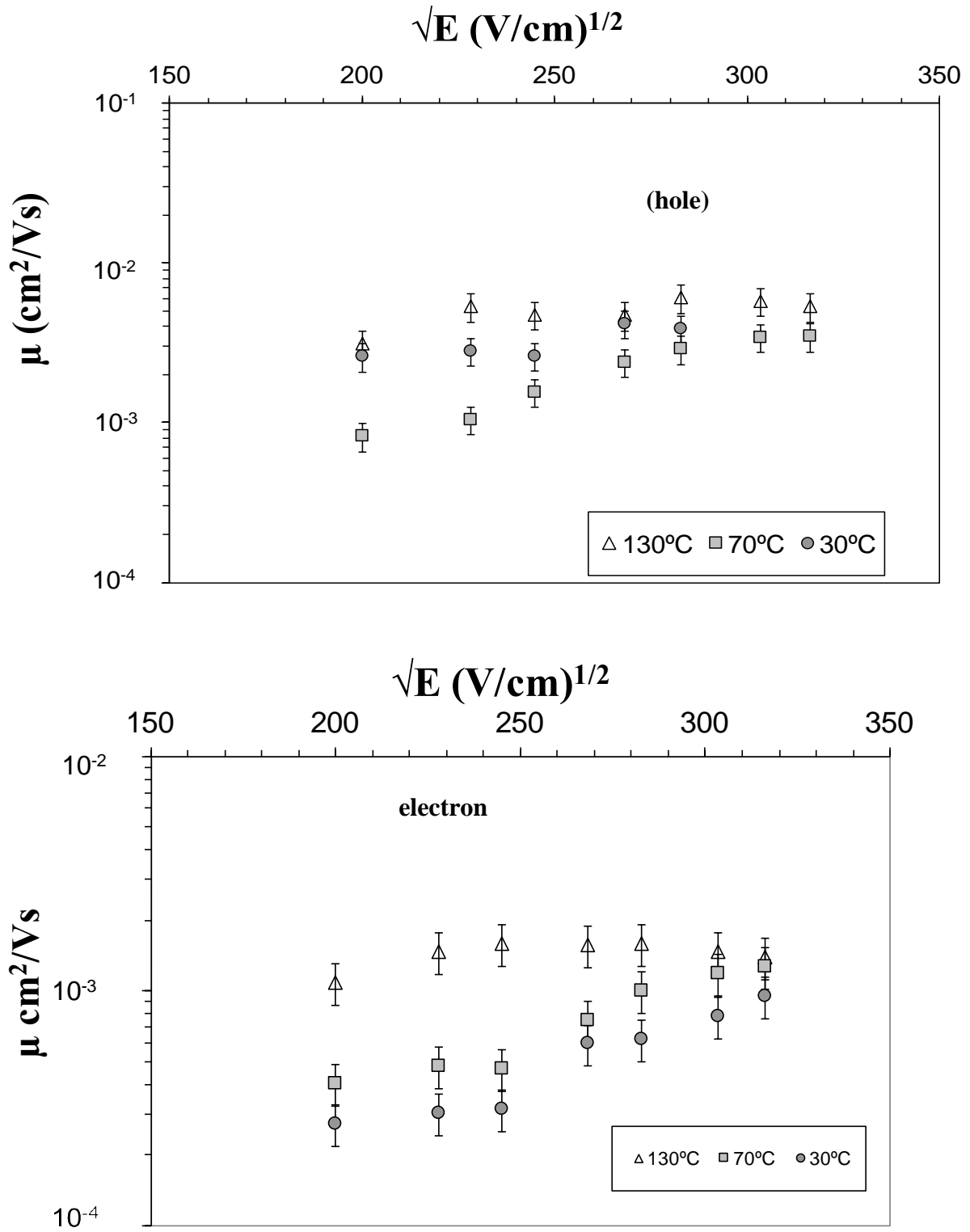


**Figure 6:** Poole-Frankel plots for hole and hole mobilities in 8GdPc<sub>2</sub> for K (circle) , Col<sub>r</sub> (rectangle) and Col<sub>h</sub> (triangle) mesophases corresponding to transition temperature of 30°C, 70°C and 130°C, respectively